Influence of cell cycle phase on calcification in the coccolithophore *Emiliania huxleyi*

Marius N. Müller, Avan N. Antia,[1] *and Julie LaRoche*
Leibniz Institute for Marine Science, Research Division: Marine Biogeochemistry, Düsternbrooker Weg 20, 24105 Kiel, Germany

Abstract

Calcification of the cosmopolitan coccolithophore species *Emiliania huxleyi* was investigated in relation to the cell division cycle with the use of batch cultures. With a 12 : 12 h light : dark cycle, the population was synchronised to undergo division as a cohort, simultaneously passing through the G1 (assimilation), S (DNA replication), and G2+M (cell division and mitosis) phases. Cell division was followed with the use of quantitative DNA staining and flow cytometry. Simultaneously, carbon-14 (^{14}C) assimilation in organic and inorganic carbon as well as cell abundance, size, and organic nitrogen content were measured at 2-h intervals. In additional experiments, changes in calcification and cell cycle stages were investigated in nitrogen-, phosphorus-, and light-limited cultures. Calcification occurred only during the G1 cell cycle phase, as seen by the very tight correlation between the percentage of cells in G1 and calcification during the dark period. When growth was limited by nitrogen, cells decreased in size, remained in the G1 phase, and showed a moderate increase in the cell-specific calcite content. Limitation of growth by phosphorus, however, caused a significant increase in cell size and a dramatic increase in cellular calcite. Light limitation, by slowing the growth rate, prolonged the time cells spent in the G1 phase with a corresponding increase in the cellular calcite content. These results help explain the differing responses of coccolithophorid growth to nitrogen, phosphorus, and light limitation.

Coccolithophores are unicellular photosynthetic algae that produce platelets of calcium carbonate, called coccoliths, that surround the cells. They are the dominant planktonic calcifiers in the present ocean and are responsible for up to 80% of global oceanic calcification (Deuser and Ross 1989; Fabry 1989) of 0.8–1.4 Pg of $CaCO_3$-C y^{-1} (Feely et al. 2004). The cosmopolitan species *Emiliania huxleyi* in particular forms huge seasonal blooms that extend over >100,000 km^2 (Brown and Yoder 1994), making it an important player in the marine environment.

Calcification plays a substantial role in the marine carbon cycle in that formation and export of calcium carbonate reduce alkalinity in the surface ocean and cause a net release of CO_2 to the atmosphere, counteracting the CO_2 drawdown by photosynthesis. Calcification thus decreases the efficiency with which the oceans' "biological pump" takes up atmospheric CO_2 (Antia et al. 2001). Hence, variations in the ratio of calcification to photosynthesis (C : P) and ratio of particulate inorganic carbon to particulate organic carbon (PIC : POC) leaving the surface ocean are important in determining the efficiency of biogenic carbon sequestration by the ocean. Additionally, because coccolith formation is negatively affected by decreasing seawater pH, changes in the abundance of calcifiers is expected because of ongoing ocean acidification (Riebesell 2004; Delille et al. 2005) with unknown effects on marine ecosystems.

Although there is no consensus as to why coccolithophores calcify (Harris 1994; Young 1994; Bratbak et al. 1996), several factors that influence the rate of calcification, as well as the ratio of calcification to photosynthesis, have been identified. In numerous controlled laboratory experiments and mesocosm and field studies, changes in calcification and the PIC : POC ratios were seen to change with dependence on light, nutrient availability, growth rate, and strain diversity (summarized in Paasche 2002). Elevated bulk calcite production and cell-specific calcium carbonate quota are found particularly under high light conditions and when phosphorus rather than nitrogen limits growth (Paasche and Brubak 1994; Riegmann et al. 2000; Zondervan 2007). Higher cell–calcite quotients also result from nitrogen limitation, but to a lesser extent (Paasche 1998).

The physiological reasons underlying these observations are unclear. Calcification is energy consuming, fueled by photosynthesis in the light and respiration in the dark (Sekino and Shiraiwa 1996). Though *E. huxleyi* calcifies primarily during the light phase of the diel cycle, cells that have been decalcified by acidification can build coccoliths when incubated in the dark, albeit at a much slower rate (Sekino and Shiraiwa 1996). In his comprehensive review of the coccolithophore *E. huxleyi*, Paasche (2002) speculated that calcification is linked to the cell division cycle, with calcification being primarily a G1 (gap 1, assimilation) process and thus reduced in the dark when dividing cells pass through the S (DNA synthesis) and G2+M (gap 2 [cell division] + mitosis) phases of division. This argument is supported by the observation that the coccolith vesicle is not present during nuclear division and is reconstituted after mitosis (van Emburg 1989). If calcification is related to the G1 phase of the cell cycle, processes arresting cells in G1, such as nutrient limitation, would cause an increase in bulk calcification.

[1] Corresponding author (aantia@ifm-geomar.de).

Acknowledgments

We thank H. Schäfer for his help with the DNA staining protocol, D. Hümmer and K. Straube for help during sampling, K. Nachtigall for PON measurements, and R. Surberg for measuring the Ca samples. We also thank two anonymous reviewers for their helpful comments.

Although the cell cycle is not well studied in phytoplankton in general, a few metabolic pathways have been linked to particular stages of the cell cycle in diatoms. Although maximal photosynthetic capacity (P^{B}_{m}) and electron transport rate (ETR_m) in diatoms is associated with the G1 phase (Claquin et al. 2004), the formation of silica frustules is linked to the G2+M stage of the division cycle (Claquin et al. 2002), during which nuclear division occurs and daughter cells are formed through cleavage of the mother cell. Here, we experimentally investigate (1) whether calcification of the coccolithophore *E. huxleyi* is confined to a specific phase of the cell division cycle, analogous to silification in diatoms, and (2) whether the cell cycle and calcification rates are affected by low nutrient and low light limitation of the growth rate.

Methods

Cultures—Monocultures of *E. huxleyi* strain CCMP 371, obtained from the Center for the Culture of Marine Phytoplankton (Bigelow Laboratory, West Boothbay Harbor, Maine), were grown at 21°C in f/50 artificial seawater (Guillard 1975), corresponding to 35.2 μmol L^{-1} NO_3 and 1.44 μmol L^{-1} PO_4, with a photon flux density of 300 μmol quanta m^{-2} s^{-1}. For the cell cycle experiment, a 12 : 12 h light : dark (LD) cycle was used to synchronize the population to undergo cell division as a cohort. To minimize the sample collection to a 12-h period, cultures were incubated in parallel incubators with a 12-h offset (i.e., 12 : 12 h LD and 12 : 12 h dark : light [DL]). During the cell cycle experiment, cultures were in the exponential growth phase. For the limitation experiment, continuous light (150 μmol quanta m^{-2} s^{-1}) was used to desynchronize cell division such that a single sample yielded the average distribution of cells in each phase of the cell cycle. Cultures were grown over at least 20 generations at the described conditions before starting the experiments.

Experimental setup—For the cell cycle experiment, an exponentially growing culture was distributed evenly in six 2-liter polycarbonate bottles, of which three were placed in each of two incubators with offset LD cycles as described above. Changes in light were set at 07:00 h and 19:00 h. The experiment started at 07:00 h and lasted for 12 h, with sampling from each bottle every 2 h. Samples were taken for cell number, cell diameter, cell cycle analysis, and carbon-14 (^{14}C) incorporation rates. Nutrient samples (NO_3, PO_4) were taken at the start and the end of the experiment. Before sampling, the bottles were rotated gently by hand to distribute cells evenly.

The limitation experiment was conducted over 13 d in 2-liter polycarbonate bottles. Nitrate and phosphate concentrations were adjusted at 30 and 4 μmol L^{-1} (N : P = 8 : 1), respectively, with the following modification: For the nitrogen limitation (N-lim), NO_3 addition was reduced to 18 μmol L^{-1} (N : P = 5 : 1), and for the phosphorus limitation (P-lim), PO_4 addition was reduced to 0.5 μmol L^{-1} (N : P = 60 : 1). The light limitation (E-lim) treatment received 50 μmol quanta m^{-2} s^{-1}. All bottles were rotated continuously once per minute by a rolling device. Cell number and cell diameter were sampled daily. Samples for particulate calcium (Ca), particulate organic nitrogen (PON), cell cycle analysis, and nutrients were taken once in the lag phase and during two time points of the exponential and stationary growth phases.

Flow cytometric determination of cellular DNA content—Samples (5 mL) were taken from each bottle and centrifuged for 10 min at 864 *g*. Supernatant was decanted, and the remaining pellets were suspended in 2 mL of pure ethanol and stored at −80°C. For analysis, samples were thawed and centrifuged for 10 min at 5,500 rpm, the supernatant was discarded, and the pellets were resuspended in phosphate-buffered saline + ethylenediamine tetra-acetic acid (5 mmol L^{-1}). This step was repeated twice to remove ethanol. Following this, 10 μL of Triton X-100 solution (Sigma-Aldrich 93443) and 6 μL of RNAse A (Sigma-Aldrich R4642) were added to permealize the cell membrane and eliminate RNA. The suspension was incubated overnight in the dark at 4°C. Intracellular DNA was stained with propidium iodide (Sigma-Aldrich P4170, emission at 617 nm) to an end concentration of 100 μg mL^{-1}. DNA was measured with a FAC-S Calibur flow cytometer (Becton Dickson) equipped with an air-cooled laser providing 15 mW at 488 nm with standard filter setup. DNA histograms were analyzed to determine the proportion of cells in different phases of the cell cycle with WinMDI freeware (J. Trotter). The G1 and the G2+M fluorescence peaks were assumed to have a Gaussian distribution, and the S phase was defined as the gap between the G1 and G2+M peaks. Half of the overlap between G1 to S and S to G2+M was assigned to each of the adjoining phases.

PON—Duplicate 35-mL subsamples from each bottle were filtered onto precombusted GF/F filters and frozen at −20°C. For PON analysis, filters were fumed over HCl for 24 h and measured with a Euro EA Elemental Analyser (Ehrhardt and Koeve 1999).

Ca—Duplicates of 35 mL were filtered from each bottle over acid-washed polycarbonate filters (poresize 0.2 μm), and the filters were stored at −20°C. Filters were put into 0.25 mol L^{-1} HCl and left for 5 min in an ultrasonic bath to dissolve $CaCO_3$. Ca was measured by inductively coupled plasma–optical emission spectrometry.

Cell counts—Cell number and cell diameter were determinated with a Coulter Counter connected to a Coulter multisizer. Analyses were performed with the MULTI 32 program (Beckton Dickson) and growth rate (μ) was calculated as

$$\mu = \frac{(\ln c_1 - \ln c_0)}{t_1 - t_0}$$

where c_0 and c_1 are the cell concentrations at time t_0 and t_1. Two-hour growth rate calculations were used to plot increments in cell number over the 12-h incubation by normalizing to a relative cell number at the start of the cell cycle experiment.

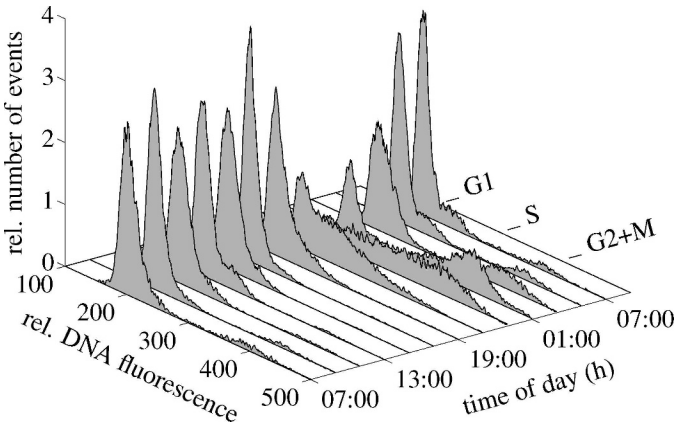

Fig. 1. DNA fluorescence histograms in 2-h intervals over the duration of the cell cycle experiment.

Nutrients—Samples (60 mL) for PO_4 and NO_3 were taken from each bottle and filtered through GF/F filters, and the filtrate was frozen in polyethylene bottles. Duplicate samples from each bottle were analyzed colorimetrically after Hansen and Koroleff (1999). Nutrient consumption of dark and light periods was calculated from the difference in the nutrient concentration at the start and the end of each period and related to the starting cell concentration of the period.

Organic and inorganic ^{14}C incorporation—Every 2 h a sample of 50 mL was taken from each bottle, spiked with 74 kBq$H^{14}CO_3$ (Hartmann Analytic MC208), and incubated in 60-mL culture flasks under 300 μmol photons m^{-2} s^{-1} for 2 h. After incubation, duplicate samples of 10 mL each were filtered onto cellulose acetate filters (poresize 0.2 μm) for total carbon incorporation, and another two subsets were filtered and afterwards rinsed with 0.1 mol L^{-1} HCl to completely remove the inorganic carbon. Independent tests for removing the inorganic carbon with fuming HCl showed that >40 min were necessary to solubilize all the $CaCO_3$. Photosynthetic carbon incorporation was estimated from ^{14}C measurements after treating the filters with HCl, and calcification was calculated from the difference of total carbon incorporation and photosynthetic incorporated carbon.

Results

Cell cycle experiment—Cell division could be followed as a cohort of cells synchronously going through DNA replication and division (Fig. 1).

During the light period, most cells (>85%) were in the G1 phase. DNA replication started after onset of darkness with a maximum number of cells accumulated in the S phase at 23:00 h. This cohort proceeded through G2+M, with a peak at 01:00 h, and underwent mitosis between 00:00 and 03:00 h. Phase durations were estimated as 19.3, 2.2, and 2.5 h for G1, S, and G2+M, respectively. Use of the frequency of dividing cell method (Carpenter and Chang 1988) for calculation of growth rate yields 1.05 d^{-1}, compared with 1.08 d^{-1} by cell count.

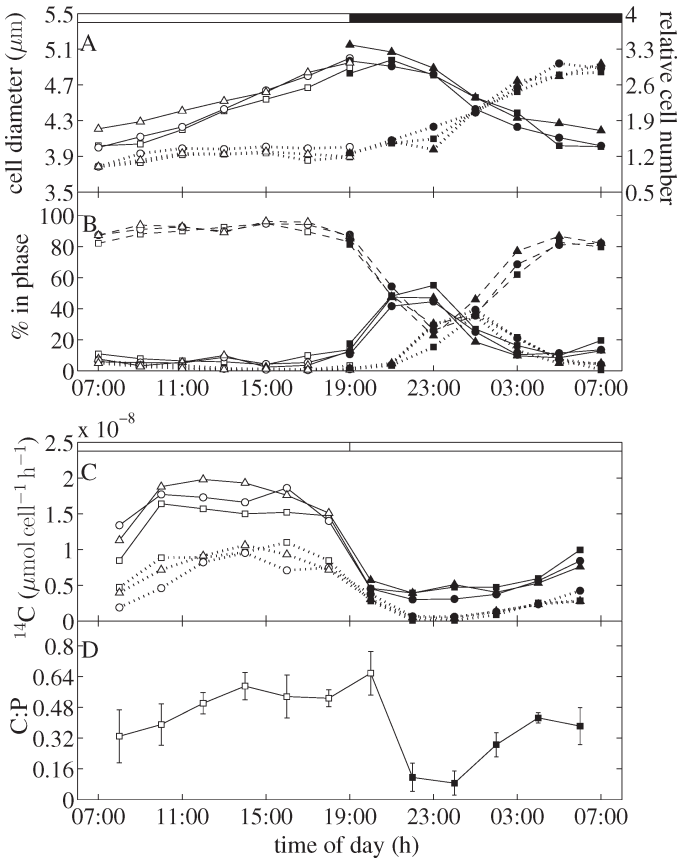

Fig. 2. Diurnal cycle relating calcification and photosynthesis to cell cycle parameters in *E. huxleyi*. Open symbols are triplicate flasks from the light period. Closed symbols are triplicate flasks from the dark period. (A) Cell diameter (solid line) and relative cell number (dotted line) in the light and dark periods. (B) Percentage of cells in each phase of the cell cycle during the light and dark periods. G1 (dashed line), S (solid line), and G2+M (dotted line). (C) ^{14}C-incorporation of organic (solid line) and inorganic carbon (dotted line) in the light. (D) Mean values of the calcification-to-photosynthesis ratio (C : P) in the light. Error bars indicate the standard error (n = 9). Open and closed bars at the top of panels A and C indicate light (open) and dark (closed) incubation.

Both cell diameter and cell number showed a clear daily cycle in all bottles (Fig. 2A). Here, relative cell number (relative to the start of the experiment) is used to balance slight differences in cell numbers between the parallel LD and DL cultures. During the light period, cell number remained constant while cell diameter increased from ~4.0 to ~4.9 μm. Cell division took place between 00:00 and 03:00 h, as seen in the increase in cell number and decrease in average cell diameter during that time.

Figure 2B shows the percentage of cells in each phase of the cell cycle through a 24-h period, demonstrating a clear progression of the cohort through division. The coefficient of variation for determination of the G1 phase ranged from 5.7% to 11.9%. The organic and inorganic ^{14}C-uptake rates (Fig. 2C) also show a diel cycle relating to the LD periodicity (recall that the samples taken from the dark were incubated in the light). The ratio of calcification to

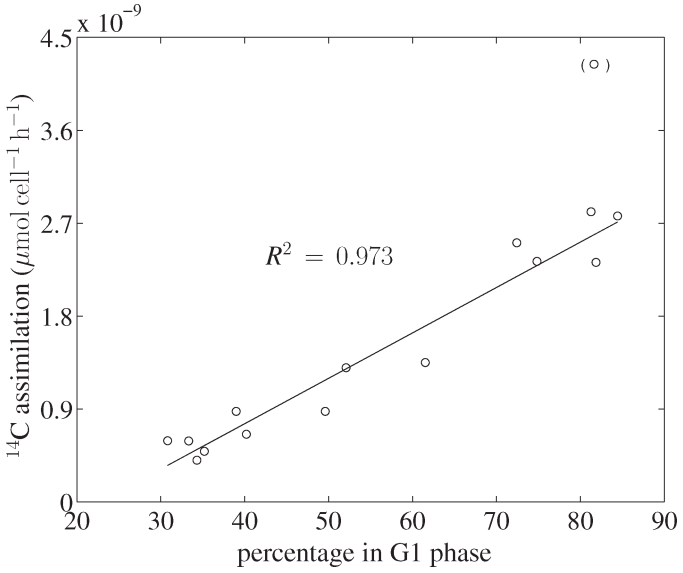

Fig. 3. ^{14}C assimilation of inorganic carbon versus percentage of cells in the G1 phase. Regression excludes the data point in brackets, $n = 14$.

photosynthesis (C : P) varied between 0.09 and 0.66, with a marked minimum between 22:00 and 00:00 h (Fig. 2D). This minimum was due to practically a cessation of calcification during the S and G2+M phases in the dark. During the dark period, the rate of calcification was very tightly and positively correlated to the proportion of cells in G1 ($r^2 = 0.97$, $n = 14$; Fig. 3), strongly suggesting that calcification is restricted to the G1 phase (only data of the dark period was correlated because of no significant changes in percent cells in G1 during the light period). A significant, negative correlation was also seen between calcification and percent cells in S ($r^2 = -0.81$, $n = 14$) and G2+M ($r^2 = -0.72$, $n = 14$). Correlation of photosynthesis and cell cycle stage G1 was lower for the dark period ($r^2 = 0.53$, $n = 14$).

Nitrogen consumption per cell in the dark period was between 45% and 90% less than in the light. The reverse was observed for phosphorus, with 34–62% less phosphorus being consumed in the light period than in the dark (Table 1). Correspondingly, there was a clear light–dark trend in the ratios of nitrogen and phosphorus uptake ($N : P_{light} = 28.2$, SEM = 5.7; $N : P_{dark} = 8.5$, SEM = 1.3).

Limitation experiment—All four treatments started with an initial cell density of 1.6×10^3 cells mL^{-1} (Fig. 4A) and

Table 1. Nitrogen and phosphorus consumption during the light and dark periods of the experiment.

	Nitrogen consumption (μmol cell^{-1} 12 h^{-1})		Phosphorus consumption (μmol cell^{-1} 12 h^{-1})	
Flask	Light	Dark	Light	Dark
1	4.36×10^{-8}	1.78×10^{-8}	3.56×10^{-9}	3.73×10^{-9}
2	7.06×10^{-8}	3.10×10^{-8}	3.37×10^{-9}	4.36×10^{-9}
3	7.18×10^{-8}	5.47×10^{-8}	1.27×10^{-9}	4.19×10^{-9}

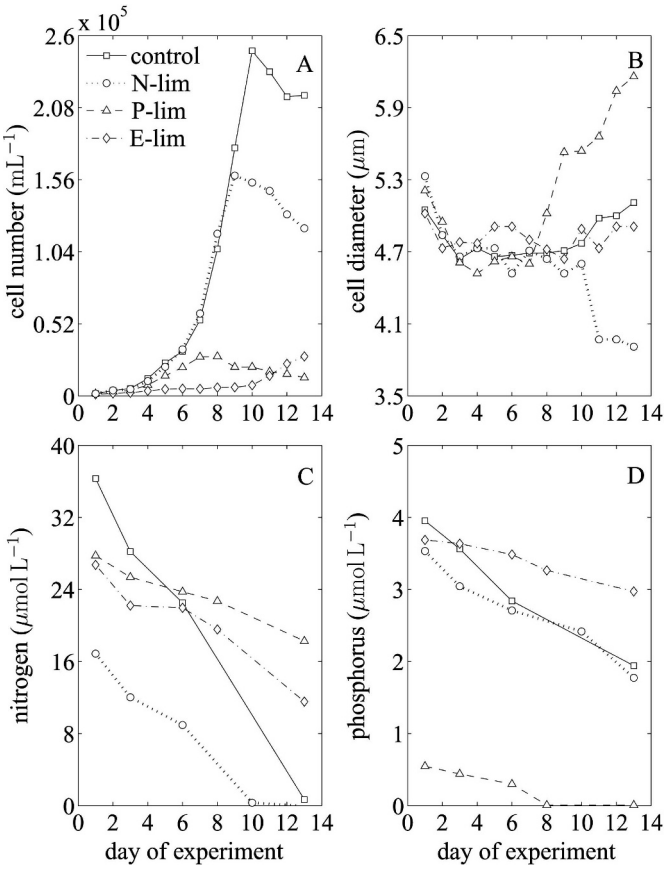

Fig. 4. Time course of nutrient and light limitation experiments. (A) Cell density, (B) average cell diameter, (C) nitrogen, and (D) phosphorus concentration.

a mean cell diameter of 4.73 μm (Fig. 4B). After a 2-d lag phase, the cells entered the exponential growth phase, in which the control, N limitation, and P limitation treatments reached a growth rate (μ) of 0.54–0.58 d^{-1}. The light-limited treatment had a mean growth rate of 0.32 d^{-1} during the entire experiment. After day 5, phosphorus was exhausted in the P-limited treatment (Fig. 4D), following which, the cells steadily increased in diameter to a mean of 6.20 μm at the end of the stationary phase (Fig. 4B). Nitrogen limitation was reached on day 7, followed by a decrease in cell diameter to 3.90 μm by day 10. Cell diameter of the control and light-limited treatments stayed nearly constant throughout the exponential growth phase. Nitrogen was exhausted between days 10 and 13 in the control culture. Thus, the data from the control beyond day 10 are not used in the compilation of Table 2.

The percentage of cells in a specific cell cycle phase changed under N and P limitation. In both cases, the proportion of cells in G1 phase rose significantly in the stationary phase (Table 2). Consequently, the percentage in S and G2+M declined. Light limitation showed no significant difference in percent cells in G1 compared with the control and nutrient limitations during the exponential growth phase.

Table 2. Growth rate (μ), particulate calcium (Ca), particulate organic nitrogen (PON), and the percentage of cells in the G1 phase of the different limitations during exponential and stationary growth phase (mean±SD, n=2).

Limitation	μ (d^{-1})	Ca (μmol $cell^{-1}$)×10^{-6}	PON (μmol $cell^{-1}$)×10^{-6}	% in G1
Exponential growth phase				
Control	0.58±0.09	2.30±1.20	0.33±0.19	75.1±2.8
N	0.58±0.16	2.04±1.09	0.25±0.14	76.3±2.6
P	0.54±0.13	2.98±0.25	0.49±0.32	74.4±2.8
E	0.34±0.15	4.53±1.68	0.61±0.34	77.2±5.2
Start of stationary growth phase				
N	—	2.59±0.01	0.10±0.01	86.3
P	—	4.53±0.03	0.26±0.01	87.6
End of stationary growth phase				
N	—	3.64±0.05	0.12±0.01	89.0
P	—	17.59±0.52	0.47±0.06	87.4

Discussion

This study shows a clear synchronization of cell division in an exponentially growing culture of *E. huxleyi*, triggered by a LD cycle, as previously reported by Jochem and Meyerdierks (1999). The synchronized cohort is seen by transition of the cells through each of the three cell cycle phases (Figs. 1, 2B) and as a steplike increase in cell number during the dark period (Fig. 2A). Illumination over several generations with continuous light leads to a desynchronization of division, and thereafter, the distribution of cells in each cell cycle stage stays constant with time (data not shown).

The very tight correlation ($r^2 = 0.97$; Fig. 3) between the percentage of cells in G1 and the rate of calcification during passage through the division cycle in the dark period leads us to conclude that calcification is largely confined to the G1 phase. Because calcification is energy intensive, cells would have an advantage by suppressing this process during cell division, when the very sensitive process of DNA replication takes place. Linschooten et al. (1991) and van Emburg (1989) have reported that during mitosis, the coccolith vesicle disappears and is only rebuilt after newly divided cells are illuminated, suggesting that, mechanistically, dividing cells are incapable of calcifying. Restriction of calcification to the G1 phase would reconcile the contradictory observations of dark calcification reported in various studies, as already postulated by Paasche (2002). Whereas numerous studies reported the phenomenon of dark calcification (even though at a greatly reduced rate) in coccolithophores (Balch et al. 1992; Paasche and Brubak 1994; Sekino and Shiraiwa 1994), Linschooten et al. (1991) have found no indication for dark calcification. Because the latter experiments were conducted in a 16 : 8 h LD cycle at a growth rate (μ) of 0.69 (one doubling per day), the whole population would pass the S and G2+M phases during the short dark period. Hence, one possible explanation for absence of dark calcification would be the lack of cells in the G1 phase during the dark period.

During passage through the division cycle, cells have differing nutrient demands. In the G1 phase, nitrogen consumption is high because cells are synthesizing and accumulating biomass. Once the cells switch into the S phase, their nitrogen requirement decreases because protein synthesis is suppressed during this phase of the cell cycle (Ronning and Lindmo 1983). This is confirmed by the lower consumption of nitrogen in the dark (Table 1). On the other hand, the data did not show significant differences in phosphorus consumption between the light and dark period (presumably because of difficulties in measuring the very small changes in value over 12 h), although a tendency for higher demand of phosphorus in the dark was seen. The resulting N : P uptake ratio is significantly lower in the dark. Riegmann et al. (2000) similarly reported a 70% lower uptake rate for nitrogen in the dark compared with the light in *E. huxleyi*. In their study, the authors did not find any DL differences in the uptake rate for phosphorus, only a higher affinity during the dark. This probably reflects the high requirement of phosphorus for nucleic acid and phospholipid membrane synthesis immediately before cell division (Geider and LaRoche 2002).

We found, under nutrient-replete conditions, that *E. huxleyi* cells only entered the cell division cycle after reaching a critical diameter in the G1 phase. This was independent of the degree of calcification because the same trend was seen in experiments conducted with naked (decalcified) *E. huxleyi* cultures (data not shown). Cell diameter could thus be a trigger to enter the S phase and hence be a potential restriction point in the cell cycle. A similar effect of cell diameter has been reported previously for yeast cells (Nurse and Fantes 1981) but has not been investigated for phytoplankton. The observed mean cell diameter before cell division during the cell cycle experiment was ~5 μm, in contrast to the average diameter during the limitation experiment of 4.75 μm. This is likely to be an effect of the desynchronization of the population under continuous light.

A clear decrease in the mean cell diameter of nitrogen-limited cells (Fig. 4B) reflects substrate limitation and lower assimilation. Conversely, phosphorus-starved but nitrogen-replete cells increase significantly in diameter because biomass buildup continues while DNA synthesis and replication are inhibited. Restriction of entry into the S phase or elongation in the absence of adequate phosphorus reserves is a successful mechanism to ensure completion of cell division and to avoid irreversible damage of nuclear material (Antia et al. 1990).

The general trends in growth rate, cellular calcite content, and cell diameters observed for the limitation experiment presented here have been documented before for *E. huxleyi* grown under light- and nutrient-limited conditions (Zondervan 2007). However, here, we further demonstrate that, as for the diurnal cycle, the increase in calcite per cell is linked to the accumulation of cells in the G1 phase.

Supporting this hypothesis, we find that under nitrogen limitation, when cell diameter drops from 4.75 to 3.90 μm, cells accumulate in the G1 phase (Table 2). However, when phosphorus limits growth rate, the cells increase in diameter to 6.20 μm while also accumulating in the G1 phase for the reasons explained above.

This results from both an increase in biomass as well as incremental coccoliths at the cell surface. The increase in cell nitrogen content (Table 2) is calculated to result in an increase in cell diameter from 4.75 to 5.60 μm, with a further 0.6-μm increase in diameter that can be ascribed to additional coccolith production.

The PON content under nitrogen limitation decreases to 0.12×10^{-6} μmol PON cell^{-1} and stays nearly constant in the stationary growth phase (Table 2). Similar changes in biomass of *E. huxleyi* under limitation has been seen in several studies (Paasche and Brubak 1994; Paasche 1998; Riegmann et al. 2000). Notably, the effect of an increase in cell diameter was also reported by Buma et al. (2000) upon irreversible damage to the DNA of *E. huxleyi* under ultraviolet-B irradiance, probably arresting the cells at the end of the G1 phase while assimilation continued.

The same average cell diameter was observed in all treatments of the limitation experiment, despite the lower growth rate observed in the light limitation treatment (0.34 d^{-1}) relative to the control and nutrient limitation treatment (0.58 d^{-1}), supporting the hypothesis of a size restriction point in the transition from the G1 to S phase. This suggests that under lower light, the length of the G1 phase is extended until the cells reach the required size to enter the cell division cycle.

According to the mechanism proposed in our study, elongation of the G1 phase under light limitation would account for the higher cellular calcite content observed under these growth conditions. However, calcite production rate (multiplying the calcite content per cell with the growth rate) is not significantly higher than calcite production in the control treatment. Given that calcification is a light-dependent process, the higher calcite content per cell in the light-limited culture might seem counterintuitive. However, this has also been reported by others before (reviewed in Zondervan 2007). This can be explained by the fact that the two light-dependent processes, photosynthesis and calcification, saturate at different light intensity thresholds, with photosynthesis requiring higher irradiance.

In addition, we hypothesize that phosphorus-limited cells, in contrast to light- and nitrogen-limited cells, can still acquire light energy required for calcification, leading to a rapid and strong rise in calcite per cell (from 2.98×10^{-6} in the exponential to 17.59×10^{-6} μmol cell^{-1} in the late stationary phase). In contrast, in the nitrogen-limited culture, the increase in cell-specific calcite content is slower and smaller (Table 2). The strong increase of calcium per cell is a commonly observed effect under phosphorus limitation (Paasche 1998; Riegmann et al. 2000). Supporting our observation of calcification being a G1 process, elongation of the time spent in G1 by the light-limited culture results in higher calcite values per cell (Table 2). Thus, elongation of the G1 phase without affecting the process of calcification would lead to an increase in cellular calcite content.

The laboratory-observed linkage of calcification with cell cycle in this study could also be true for natural populations, such as when a bloom of *E. huxleyi* produces excess coccoliths, forming "white waters" in the stationary growth phase. Natural blooms of *E. huxleyi* in temperate regions might be limited primarily by nitrogen, especially considering the higher affinity of this species for phosphorus than for nitrogen. Despite this, Nanninga and Tyrrell (1996) identify *E. huxleyi* blooms to be associated with high-light and phosphorus-poor environments, as well as a shallow mixed layer depth (Raitsos et al. 2006), emphasing that the immediate control of *E. huxleyi* growth and calcification still needs to be more closely elucidated. Alteration in cell diameter of natural populations upon onset of nutrient limitation can be relatively easily measured by flow cytometry and would provide a means of differentiating between N and P limitations in situ.

In addition to the effect of macronutrient limitation on the cell cycle, micronutrient limitation should be considered to be a factor that could influence the cell cycle. For example, Schulz et al. (2004) reported high calcium carbonate per cell of *E. huxleyi* under zinc limitation. This effect could be similar to phosphorus limitation in that zinc is required in so-called zinc finger proteins, which are highly involved in DNA transcription, and is a cofactor for alkaline phosphatase, an enzyme involved in organic phosphorus assimilation. Thus, we suggest that zinc limitation could arrest the cells in the late G1 phase, resulting in an increase in net calcite content per cell. The method presented here is easily applicable to natural *E. huxleyi* populations and could be used to determine the mechanistic basis of changes of calcification in the field.

References

Antia, A. N., E. J. Carpenter, and J. Chang. 1990. Species-specific phytoplankton growth rates via diel DNA synthesis cycles. III. Accuracy of growth rate measurement in the dinoflagellate *Prorocentrum minimum*. Mar. Ecol. Prog. Ser. **63:** 273–279.

———, and others. 2001. Basin-wide particulate carbon flux in the Atlantic Ocean: Regional export patterns and potential for atmospheric CO_2 sequestration. Glob. Biogeochem. Cycles **15:** 845–862.

Balch, W., P. Holligan, and K. Kilpatrick. 1992. Calcification, photosynthesis and growth of the bloom-forming coccolithophore, *Emiliania huxleyi*. Cont. Shelf Res. **12:** 1352–1374.

Bratbak, G., W. Wilson, and M. Heldal. 1996. Viral control of *Emiliania huxleyi* blooms? J. Mar. Syst. **9:** 78–81.

Brown, C., and J. Yoder. 1994. Coccolithophorid blooms in the global ocean. J. Geophys. Res. (C) **99:** 7467–7482.

Buma, A., T. v. Oijen, W. v. d. Poll, M. Veldhuis, and W. Gieskes. 2000. The sensitivity of *Emiliania huxleyi* (Prymnesiophyceae) to ultraviolet-B radiation. J. Phycol. **36:** 296–303.

Carpenter, E., and J. Chang. 1988. Species-specific phytoplankton growth rates via diel DNA synthesis cycles. I. Concept of the method. Mar. Ecol. Prog. Ser. **43:** 105–111.

Claquin, P., J. Kromkamp, and V. Martin-Jézéquel. 2004. Relationship between photosynthetic metabolism and cell cycle in a synchronized culture of the marine alga *Cylindrotheca fusiformes* (Bacillariophyceae). Eur. J. Phycol. **39:** 33–41.

———, V. Martin-Jézéquel, J. Kromkamp, M. Veldhuis, and G. Kraay. 2002. Uncoupling of silicon compared with carbon and nitrogen metabolisms and the role of the cell cycle in continuous cultures of *Thalassiosira pseudonana* (Bacillariophyceae) under light, nitrogen and phosphorus control. J. Phycol. **38:** 922–930.

Delille, B., and others. 2005. Response of primary production and calcification to changes of pCO_2 during experimental blooms of the coccolithophorid *Emiliania huxleyi*. Glob. Biogechem. Cycles **19:** GB2023, doi:10.1029/2004GB002318.

Deuser, W., and E. Ross. 1989. Seasonally abundant planktonic-foraminifera of the Sargasso Sea: Succession, deep-water fluxes, isotopic compositions and paleoceanographic implications. J. Foraminifer. Res. **19:** 268–293.

Ehrhardt, M., and W. Koeve. 1999. Determination of particulate organic carbon and nitrogen, p. 437–444. *In* K. Grasshoff, K. Kremling and M. Erhardt [eds.], Methods of seawater analysis, 3rd ed. Wiley-VCH.

Fabry, V. 1989. Aragonite production by pteropod mollusks in the subantarctic Pacific. Deep-Sea Res. **36:** 1735–1751.

Feely, R., C. Sabine, K. Lee, W. Berelson, J. Kleypas, V. Fabry, and F. Millero. 2004. Impact of anthropogenic CO_2 on the $CaCO_3$ system in the ocean. Science **305:** 362–366.

Geider, R., and J. LaRoche. 2002. Redfield revisited: Variability of C : N : P in marine microalgae and its biochemical basis. Eur. J. Phycol. **37:** 1–17.

Guillard, R. 1975. Culture of phytoplankton for feeding marine invertebrates, p. 26–60. *In* W. Smith and M. Chanley [eds.], Culture of marine invertebrates. Plenum.

Hansen, H. P., and F. Koroleff. 1999. Determination of nutrients, p. 159–226. *In* K. Grasshoff, K. Kremling and M. Erhardt [eds.], Methods of seawater analysis, 3rd ed. Wiley-VCH.

Harris, R. 1994. Zooplankton grazing on the coccolithophore *Emiliania huxleyi* and its role in inorganic carbon flux. Mar. Biol. **119:** 431–439.

Jochem, F., and D. Meyerdierks. 1999. Cytometric measurement of the DNA cell cycle in the presence of chlorophyll autofluorescence in marine eukaryotic phytoplankton by the blue-light excited dye YOYO-1. Mar. Ecol. Prog. Ser. **185:** 301–307.

Linschooten, C., J. D. L. van Bleijswijk, P. R. van Emburg, J. P. M. de Vrind, E. S. Kempers, P. Westbroek, and E. W. de Vrind-de Jong. 1991. Role of the light–dark cycle and medium composition on the production of coccoliths by *Emiliania huxleyi* (Haptophyceae). J. Phycol. **27:** 82–86.

Nanninga, H. J., and T. Tyrrell. 1996. Importance of light for the formation of algal blooms by *Emiliania huxleyi*. Mar. Ecol. Prog. Ser. **136:** 195–203.

Nurse, P., and P. A. Fantes. 1981. The cell cycle, p. 85–88. *In* P. C. L. John [ed.], The cell cycle. Press Syndicate of the University of Cambridge.

Paasche, E. 1998. Roles of nitrogen and phosphorus in coccolith formation in *Emiliania huxleyi* (Prymnesiophyceae). Eur. J. Phycol. **33:** 33–42.

———. 2002. A review of the coccolithophorid *Emiliania huxleyi* (Prymnesiophyceae), with particular reference to growth, coccolith formation, and calcification–photosynthesis interactions. Phycologia **40:** 503–529.

———, and S. Brubak. 1994. Enhanced calcification in the coccolithophorid *Emiliania huxleyi* (Haptophyceae) under phosphorus limitation. Phycologia **33:** 324–330.

Raitsos, D. E., S. J. Lavender, Y. Pradhan, T. Tyrell, P. C. Reid, and M. Edwards. 2006. Coccolithophore bloom size variation in response to the regional environment of the subarctic North Atlantic. Limnol. Oceanogr. **51:** 2122–2130.

Riebesell, U. 2004. Effects of CO_2 enrichment on marine phytoplankton. J. Oceanogr. **60:** 719–729.

Riegmann, R., W. Stolte, A. Noordeloos, and D. Slezak. 2000. Nutrient uptake and alkaline phosphatase (EC 3:1:3:1) activity of *Emiliania huxleyi* (Prymnesiophyceae). J. Phycol. **36:** 87–96.

Ronning, O., and T. Lindmo. 1983. Progress through G1 and S in relation to net protein accumulation in human NHIK 3025 cells. Exp. Cell Res. **144:** 171–179.

Schulz, K., I. Zondervan, L. Gerringa, K. Timmermans, M. Veldhuis, and U. Riebesell. 2004. Effect of trace metal availability on coccolithophorid calcification. Nature **430:** 673–676.

Sekino, K., and Y. Shiraiwa. 1994. Accumulation and utilization of dissolved inorganic carbon by a marine unicellular coccolithophorid, *Emiliania huxleyi*. Plant Cell Physiol. **35:** 353–361.

———, and ———. 1996. Evidence for the involvement of mitochondrial respiration in calcification in a marine coccolithophorid, *Emiliania huxleyi*. Plant Cell Physiol. **37:** 1030–1033.

van Emburg, P. 1989. Coccolith formation in *Emiliania huxleyi*. Ph.D. thesis, Leiden University.

Young, J. 1994. Functions of coccoliths, p. 63–82. *In* A. Winter and W. Siesser [eds.], Coccolithophores. Cambridge University Press.

Zondervan, I. 2007. The effect of light, macronutrients, trace metals and CO_2 on the production of calcium carbonate and organic carbon in coccolithophores—a review. Deep-Sea Res. II **41:** 521–537.

Received: 12 March 2007
Accepted: 26 September 2007
Amended: 9 October 2007